Contact formulation via a velocity description allowing efficiency improvements in frictionless contact analysis

Alexander Konyukhov, Karl Schweizerhof, Matthias Harnau
Universität Karlsruhe, Institut für Mechanik

Institut für Mechanik
Kaiserstr. 12, Geb. 20.30
76128 Karlsruhe
Tel.: +49 (0) 721/ 608-2071
Fax: +49 (0) 721/ 608-7990
E-Mail: ifm@uni-karlsruhe.de
www.ifm.uni-karlsruhe.de

Contact formulation via a velocity description allowing efficiency improvements in frictionless contact analysis

A. Konyukhov, K. Schweizerhof

2005

ABSTRACT

A velocity description, based on the consideration of contact from the surface geometry point of view, is used for a consistent formulation of contact conditions and for the derivation of the corresponding tangent matrix. Within this approach differential operations are treated as covariant derivatives in the local surface coordinate system. The main advantage is a more algorithmic and geometrical structure of the tangent matrix, which consists of a "main", a "rotational" and a pure "curvature" term. Each part of the tangent matrix contains the information either about the internal geometry of the contact surface or about the change of the geometry during incremental loading and can be estimated in a norm during the analysis. Representative examples with contact and bending of shells modelled with linear and quadratic elements over some classical second order geometrical figures serve to show situations where keeping all parts of the tangent matrix is not necessary.

Keywords

Contact problem, Velocity description, Covariant differential operations, Tangent matrix, Penalty method.

1 Introduction

From the variety of methods which are mainly used for the solution of contact problems, the "master-slave" concept is one of the most robust methods. This concept is based on the determination of the penetration of the "slave" surface, represented by "slave" nodes, resp. points, into a "master" surface. The penetration can be used for regularization methods like the penalty method and the Augmented Lagrange multiplier method. The penalty method see e.g. Wriggers and Simo [16], Laursen [7] and an extensive theoretical discussion in Kikuchi and Oden [6] leads to the exact solution in the limit when the penalty approaches infinity. As an improvement, concerning the satisfaction of impenetrability, the Augmented Lagrange method has been proposed and developed for contact problems by Wriggers, Simo and Taylor [15], Simo and Laursen [13], Pietrzak and Curnier [12]. A contemporary and comprehensive review about contact problems in general can be found in the books of Wriggers [19] and Laursen [9].

In nonlinear contact problems the penetration is a function of the current geometry and it is used for the "constitutive" model of the contact tractions. For the solution of the nonlinear

equilibrium equations by a Newton method the corresponding equations have to be linearized. The correct linearization, taking, in particular, also algorithmic aspects into account, is called consistent linearization. This procedure was considered by Wriggers and Simo [16] for the 2D case, where the penalty functional has been linearized in the global coordinate system directly. Parisch [11] developed the consistent linearization for the 3D case also in global coordinates and used equations based on an orthogonal projection of the "slave" node onto the "master" surface to get convective coordinate increments during linearization. This approach was generalized for the linearization procedure in the local surface coordinate system by Simo and Laursen [13]. In both contributions, the solution of the projection problem for every "slave" node and the consistent linearization of the global equations were considered together in one step making it difficult to distinguish the different contributions to e.g. the stiffness matrix.

In the alternative approach considered in the following, the coordinate increment vector can be treated as a velocity vector during linearization, see Bonet and Wood [1], and the linearization itself can be treated as a covariant differential operation in the local surface coordinate system, see Marsden and Hughes [10]. The main approach of the proposed velocity description is to consider the global linearization separately from the local "slave" node searching procedure and derive linearized equations from kinematic equations in the local surface coordinate system. Focusing on frictionless contact, it leads to a very simple structure of the tangent matrix for the contact element, which is naturally divided into three parts. The first "main" part, or the constitutive part, consists of the tensor product of surface normal vectors only, while the second "rotational" part contains information about rotations of the contact element during the iteration process and the third "pure curvature" part contains the curvature tensor of the "master" surface.

For an extensive test of the proposed technique numerical examples with curved surfaces are presented. These tests serve to check the influence of different parts of the contact matrix on convergence within a nonlinear solution process. Two surfaces of second order (cylinder and sphere) have been chosen for this purpose. So-called "solid-shell"elements with various orders of approximation are used to model the shell structures, see [3], [4] and [5].

2 Contravariant formulation of contact conditions and linearization

We introduce two coordinate systems: a reference global coordinate system for the finite element discretization only and a spatial local surface coordinate system in the contact consideration. All geometric properties of the element as well as the differential operations will be described in the local coordinate system.

2.1 Geometry of the contact condition

A surface 2D coordinate system is usually defined to describe the surface geometry. In addition, a special 3D local coordinate system which is related to this surface can be constructed to describe any spatial object. This system will be used to define any characteristics that belongs to the surface as well as to transfer the result of the linearization into the global coordinate system for the purpose of a finite element implementation. All geometric and kinematic characteristics of the contact are investigated in the local coordinate system. First, all necessary operations in the surface coordinate system are described. For this a surface element (Fig.1), the so-called "master" element, is considered, which is parameterized by local coordinates ξ^1, ξ^2. $\mathbf{r}$ is a vector, describing an arbitrary point on the surface. It has the following form

$$\mathbf{r} = \sum_k N_k(\xi^1, \xi^2)\mathbf{x}^{(k)}. \tag{1}$$

where $N_k(\xi^1, \xi^2)$, $k = 1, 2, .., n$ are later the shape functions of e.g. finite elements.

Though a rather general description is given, we present for implementation purposes the expression for a 4-node bilinear surface element in detail. The approximation for this element can be written as

$$\mathbf{r} = \sum_{k=1}^{4} N_k(\xi^1, \xi^2)\mathbf{x}^{(k)} = \frac{1}{4}\sum_{k=1}^{4}(1 + \xi^1\xi^{(k)})(1 + \xi^2\xi^{(k)})\mathbf{x}^{(k)}. \tag{2}$$

In order to describe the geometry of the surface element from the internal differential geometry point of view, surface tangent vectors $\mathbf{r}_{,i}, \quad i = 1, 2$ have to be specified

$$\mathbf{r}_{,1} = \frac{\partial \mathbf{r}}{\partial \xi^1}, \quad \mathbf{r}_{,2} = \frac{\partial \mathbf{r}}{\partial \xi^2}. \tag{3}$$

The normal surface vector is computed as a cross product of the tangent vectors

$$\mathbf{n} = \frac{\mathbf{r}_{,1} \times \mathbf{r}_{,2}}{|\mathbf{r}_{,1} \times \mathbf{r}_2|}. \tag{4}$$

The surface vectors $\mathbf{r}_{,1}, \ \mathbf{r}_{,2}$ define a surface coordinate system, while the normal $\mathbf{n}$ is used to describe geometrical properties of the surface and to construct a local 3D coordinate system as well. The coordinate vectors serve to obtain two fundamental tensors of the surface: the first (also called a metric tensor) and the second fundamental tensors [2] (also called a curvature tensor). The covariant components of the metric tensor are defined by the dot product of the base surface vectors

$$a_{ij} = \mathbf{r}_{,i} \cdot \mathbf{r}_{,j}, \quad i, j = 1, 2. \tag{5}$$

Assuming invertibility of the metric tensor (5), the contravariant components of the metric tensor a^{ij} can be defined as

$$a^{ij} : \quad \frac{1}{a}\begin{bmatrix} a_{22} & -a_{12} \\ -a_{12} & a_{11} \end{bmatrix}, \quad a = det(a_{ij}) = a_{11}a_{22} - (a_{12})^2 \tag{6}$$

Covariant components of the second fundamental tensor are given as a dot product of the second derivative of the vector $\mathbf{r}$ and the normal $\mathbf{n}$

$$h_{ij} = \mathbf{r}_{ij} \cdot \ \mathbf{n}, \tag{7}$$

and contravariant components are defined as a double summation with the contravariant components of the metric tensor given as

$$h^{ij} = h_{kl}a^{ik}a^{jl}. \tag{8}$$

The formulae of partial derivatives of the base vectors are necessary to describe any differential operation in the local surface coordinate system. The Weingarten formula [2] for the derivative of the normal vector $\mathbf{n}$

$$\mathbf{n}_i = -h_{ij}a^{jk}\mathbf{r}_k = -h_i^k\mathbf{r}_k \tag{9}$$

and the Gauss-Kodazzi formula [2], for the derivatives of the surface vectors $\mathbf{r}_{,i}$,

$$\mathbf{r}_{ij} = \Gamma_{ij}^k\mathbf{r}_k + h_{ij}\mathbf{n} \tag{10}$$

are among them. In the last equation (10) Γ_{ij}^k are the Christoffel symbols, defined as

$$\Gamma_{ij}^k = \mathbf{r}_{ij} \cdot \mathbf{r}^k = \mathbf{r}_{ij} \cdot \mathbf{r}_m a^{mk}. \tag{11}$$

2.1.1 Projection of the contact node vector onto the master surface.

The penetration is computed by a projection procedure, see [19], [9]. Let $\mathbf{r}_s$ be a position vector of a "slave" node in the 3D space and $\mathbf{r}$ its projection onto the "master" surface. The standard closest point projection procedure leads then to the following extremal problem

$$||(\mathbf{r}_s - \mathbf{r})|| \to \min \implies (\mathbf{r}_s - \mathbf{r}) \cdot (\mathbf{r}_s - \mathbf{r}) \to \min . \tag{12}$$

As is well known, the solution of this problem can be achieved by the application of a Newton procedure for the function

$$F(\xi^1, \xi^2) = (\mathbf{r}_s - \mathbf{r})^2 \tag{13}$$

$$\Delta\xi_{n+1} = \begin{pmatrix} \Delta\xi^1_{n+1} \\ \Delta\xi^2_{n+1} \end{pmatrix} = -(F'')^{-1}_n \; F'_n \tag{14}$$

$$\xi_{n+1} = \xi_n + \Delta\xi_{n+1}$$

The first derivative with respect to the surface coordinates in the form of

$$F' = \begin{pmatrix} \frac{\partial F}{\partial \xi^1} \\ \frac{\partial F}{\partial \xi^2} \end{pmatrix} = -2 \cdot \begin{pmatrix} \mathbf{r}_{,1} \cdot (\mathbf{r}_s - \mathbf{r}) \\ \mathbf{r}_{,2} \cdot (\mathbf{r}_s - \mathbf{r}) \end{pmatrix} \tag{15}$$

must be finally zero. The second derivative has the form

$$F'' = \begin{bmatrix} \frac{\partial^2 F}{\partial \xi^1 \partial \xi^1} & \frac{\partial^2 F}{\partial \xi^1 \partial \xi^2} \\ \frac{\partial^2 F}{\partial \xi^2 \partial \xi^1} & \frac{\partial^2 F}{\partial \xi^2 \partial \xi^2} \end{bmatrix} = 2 \cdot \begin{bmatrix} \mathbf{r}_{,1} \cdot \mathbf{r}_{,1} - \mathbf{r}_{,11}(\mathbf{r}_s - \mathbf{r}) & \mathbf{r}_{,1} \cdot \mathbf{r}_{,2} - \mathbf{r}_{,12}(\mathbf{r}_s - \mathbf{r}) \\ \mathbf{r}_{,2} \cdot \mathbf{r}_{,1} - \mathbf{r}_{,12}(\mathbf{r}_s - \mathbf{r}) & \mathbf{r}_{,2} \cdot \mathbf{r}_{,2} - \mathbf{r}_{,22}(\mathbf{r}_s - \mathbf{r}) \end{bmatrix} =$$

$$= 2 \cdot \begin{bmatrix} a_{11} - \mathbf{r}_{11}(\mathbf{r}_s - \mathbf{r}) & a_{12} - \mathbf{r}_{12}(\mathbf{r}_s - \mathbf{r}) \\ a_{21} - \mathbf{r}_{22}(\mathbf{r}_s - \mathbf{r}) & a_{22} - \mathbf{r}_{22}(\mathbf{r}_s - \mathbf{r}) \end{bmatrix} \tag{16}$$

2.1.2 Spatial local coordinate system and internal geometry of the element

Now we construct a special local coordinate system, introducing the third coordinate ξ^3 in the direction of the surface normal $\mathbf{n}$, and keeping a surface point $\mathbf{r}(\xi^1, \xi^2)$ as a projection of the "slave" point. Any spatial vector in this system can be written as

$$\mathbf{r}_s(\xi^1, \xi^2, \xi^3) = \mathbf{r}(\xi^1, \xi^2) + \xi^3 \mathbf{n}. \tag{17}$$

One should notice that the projection procedure is taken into account within our local coordinate system. The Lie type derivative in the form of a covariant derivative [10] is used for any differential operation on the surface. If e.g. $\mathbf{a}$ is a vector which is defined in the local coordinate system, then its material time derivative is defined as

$$\frac{d}{dt}\mathbf{a} = (\frac{\partial a^i}{\partial t} + \nabla_j a^i \dot{\xi^j})\mathbf{r}_{,i}, \tag{18}$$

where the term $\nabla_j a^i$ is a covariant derivative of the contravariant component a^i

$$\nabla_j a^i = \frac{\partial a^i}{\partial \xi^j} + a^k \Gamma^i_{jk}. \tag{19}$$

The "slave" point in the local coordinate system (17) has the local coordinate ξ^3 (Fig. 1). We now consider the motion of the "slave" point S in the local coordinate system, assuming

that the "master" surface is moving, i.e. the surface vector $\mathbf{r}(t, \xi^1, \xi^2, \xi^3)$ as well as the normal $\mathbf{n}(t, \xi^1, \xi^2, \xi^3)$ are time dependent. Within a static process, the time t is an incremental load parameter. Then the full time derivative becomes

$$\frac{d}{dt}\mathbf{r}_s(t, \xi^1, \xi^2, \xi^3) = \frac{d}{dt}\mathbf{r} + \frac{d}{dt}(\mathbf{n}\xi^3) = \tag{20}$$

$$= \frac{\partial \mathbf{r}}{\partial t} + \frac{\partial \mathbf{r}}{\partial \xi^j}\dot{\xi}^j + \frac{\partial \mathbf{n}}{\partial t}\xi^3 + \mathbf{n}\dot{\xi}^3 + \frac{\partial \mathbf{n}}{\partial \xi^j}\xi^3\dot{\xi}^j, \quad j = 1, 2.$$

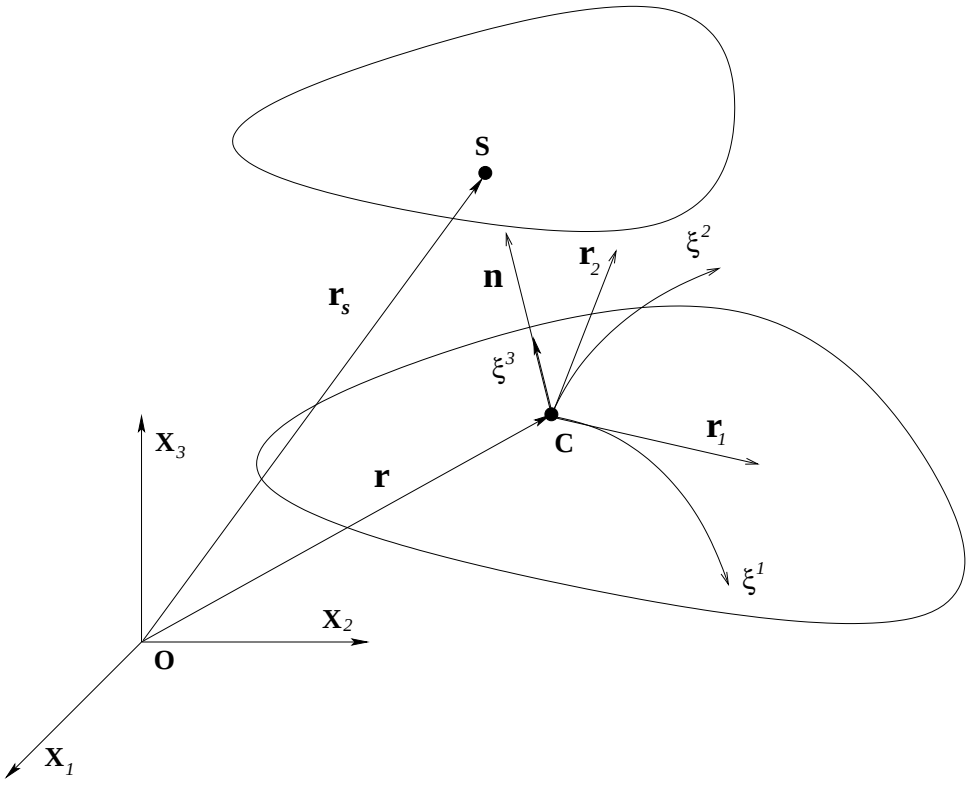

Figure 1: Definition of coordinate systems

Let a point C be a projection point of the "slave" node onto the master surface. Denote the translation velocity of the point C as $\mathbf{v} = \dfrac{\partial \mathbf{r}}{\partial t}$ and the velocity of the "slave" point as $\mathbf{v}_s = \dfrac{d}{dt}\mathbf{r}_s(t, \xi^1, \xi^2, \xi^3)$. Then equation (20) has the following form, using the Weingarten formula (9),

$$\mathbf{v}_s = \mathbf{v} + \xi^3\frac{\partial \mathbf{n}}{\partial t} + \mathbf{n}\dot{\xi}^3 + (\mathbf{r}_{,j} - \xi^3 h^i_j \mathbf{r}_{,i})\dot{\xi}^j, \quad i, j = 1, 2, \tag{21}$$

where h^i_j are mixed components of the curvature tensor.

The difference between the velocity $\mathbf{v}_s$ of "slave" point S and the velocity of point C is a relative velocity $\mathbf{v}^{rel}$ of the "slave" point, or in other words, the velocity of point S as it can be seen from point C. In order to define its projection in the local coordinate system, the dot product of the relative velocity $\mathbf{v}^{rel}$ and the coordinate vector $\mathbf{r}_{,i}$ is taken

$$(\mathbf{v}_s - \mathbf{v}) \cdot \mathbf{r}_{,i} = (a_{ij} - \xi^3 h_{ij})\dot{\xi}^j + \xi^3(\frac{\partial \mathbf{n}}{\partial t} \cdot \mathbf{r}_{,i}), \tag{22}$$

where a_{ij} are the components of the metric tensor. Therefore, the convective velocity is defined as

$$\dot{\xi}^j = \hat{a}^{ij}[(\mathbf{v}_s - \mathbf{v}) \cdot \mathbf{r}_{,i} - \xi^3(\frac{\partial \mathbf{n}}{\partial t} \cdot \mathbf{r}_{,i})] \tag{23}$$

where $\hat{a}^{ij}$ are contravariant components of the tensor with components $a_{ij} - \xi^3 h_{ij}$.

The third coordinate ξ^3 is a penetration

$$\xi^3 = g = (\mathbf{r}_s - \mathbf{r}) \cdot \mathbf{n}. \tag{24}$$

The scalar product of the normal $\mathbf{n}$ and the equation (21) gives the time derivative of the penetration

$$\dot{\xi}^3 = (\mathbf{v}_s - \mathbf{v}) \cdot \mathbf{n}. \tag{25}$$

All further considerations are based on the following assumption: Only the contact problem is considered, but not the motion and deformation of the two body system connected by means of the normal vector with coordinate ξ^3. The penetration is assumed to be very small, as usual during the solution of contact problems. Further, the global iteration procedure for the solution leads to a decreasing value of the penetration g. Thus, the convective velocity, with the additional assumption $\xi^3 = 0$, can be defined in the form

$$\dot{\xi}^j = a^{ij}(\mathbf{v}_s - \mathbf{v}) \cdot \mathbf{r}_{,i}. \tag{26}$$

This definition of the convective velocity (26) on the tangent plane allows to consider the contact kinematics on the master surface only and to exploit the differential geometry of the surface during further considerations. The formula in eq. (26) was mentioned in Wriggers [18] as a possible simplifiction as well. Here we show that from a mathematical point of view this simplifiction leads to a consistent expression of the contact integral and, as it can be seen from numerical results, also leads to high numerical efficiency.

In order to estimate the difference between the exact definition in equation (23) and the proposed form (26), a series expansion of A^{ij} assuming ξ^3 as a small parameter is performed. Suppose A is a metric tensor with components a_{ij}, H is a curvature tensor with components h_{ij} and tensor $\hat{A}$ with components $a_{ij} - \xi^3 h_{ij}$

$$\hat{A}^{-1} = (A - \xi^3 H)^{-1} = A^{-1} + \xi^3 A^{-1} H A^{-1} + \mathcal{O}((\xi^3)^2) \tag{27}$$

where A^{-1} is the contravariant metric tensor with components a^{ij}. Then the convective velocity has the following form:

$$\dot{\xi}^j = a^{ij}(\mathbf{v}_s - \mathbf{v}) \cdot \mathbf{r}_i + \xi^3 \left[a^{ik} a^{mj} h_{km} (\mathbf{v}_s - \mathbf{v}) \cdot \mathbf{r}_i - a^{ij} \dot{\mathbf{n}} \cdot \mathbf{r}_{,i} \right] + \mathcal{O}((\xi^3)^2) \tag{28}$$

It is obvious that eqn. (26) describes the constant main part of the full equation.

3 Weak formulation of the contact conditions.

For the complete description contact tractions $\mathbf{T}_1$, $\mathbf{T}_2$ on the surfaces s_1 and s_2 in the current configuration have to be considered, $\delta\mathbf{u}$ is then the variation of the displacement field on the surface. The virtual work δW_c of the contact tractions is obtained by the following surface integral

$$\delta W_c = \int_{s_1} \mathbf{T}_1 \cdot \delta\mathbf{u}_1 ds_1 + \int_{s_2} \mathbf{T}_2 \cdot \delta\mathbf{u}_2 ds_2 \tag{29}$$

which must be added to the global work of the internal and external forces. Due to the equilibrium equation at the contact boundary, $\mathbf{T}_1 ds_1 = -\mathbf{T}_2 ds_2$, equation (29) can be written as

$$\delta W_c = \int_{s_1} \mathbf{T}_1 \cdot (\delta \mathbf{u}_1 - \delta \mathbf{u}_2) ds_1 \tag{30}$$

Up to now, one surface has to be specified as the "master" and the other one as the "slave" surface. The contact integral is computed over the "slave" surface. It can be computed using quadrature formulae [9] or, in simple cases, nodal quadrature [17]. With s_1 as the "slave" surface, the redefined previous notation leads to $\delta \mathbf{u}_1 = \delta \mathbf{r}_s$ as the variation of the "slave" point and $\delta \mathbf{u}_2 = \delta \mathbf{r}$ as a projection of the the variation of "slave" point onto the "master" surface.

The traction vector in the local coordinate system can be split into a normal and into a tangential part

$$\mathbf{T}_1 \equiv \mathbf{T} = N\mathbf{n} + T^i \mathbf{r}_{,i}. \tag{31}$$

Here the traction vector is defined as a contravariant vector. An equation for the variation is derived following the kinematic equation (21):

$$\delta \mathbf{r}_s - \delta \mathbf{r} = (\mathbf{r}_{,j} - \xi^3 h^i_j \mathbf{r}_{,i}) \delta \xi^j + \mathbf{n} \delta \xi^3 + \xi^3 \delta \mathbf{n} \tag{32}$$

It should be mentioned, that the variation itself is time independent. Then the contact integral (30) can be written in the following form:

$$\delta W_c = \int_s N \delta \xi^3 ds + \int_s [a_{ij} T^i \delta \xi^j + \xi^3 T^i (\delta \mathbf{n} \cdot \mathbf{r}_{,i} - h^k_j a_{ik} \delta \xi^j)] ds \tag{33}$$

with

$$\delta \xi^3 = \delta g = (\delta \mathbf{r}_s - \delta \mathbf{r}) \cdot \mathbf{n}. \tag{34}$$

In most formulations (see Wriggers [19] and Laursen [9]), it is assumed that the virtual work is considered on the surface, i.e. $\xi^3 = 0$. Therefore, the contact integral (33) can be reduced to the following form:

$$\begin{aligned} \delta W_c &= \int_s N \delta g ds + \int_s a_{ij} T^i \delta \xi^j ds = \\ &= \int_s N (\delta \mathbf{r}_s - \delta \mathbf{r}) \cdot \mathbf{n} ds + \int_s T^i (\delta \mathbf{r}_s - \delta \mathbf{r}) \cdot \mathbf{r}_{,i} ds \end{aligned} \tag{35}$$

This form (35) is mostly used in contact mechanics. Therefore it appears contradictory to use equations for the convective velocity in the full form of eqn. (23) with the reduced form of the contact integral (35). One can show that the contact integral in the form (35) is the main part of the full form (33) after consistent expansion into a Taylor series with the small parameter ξ^3, i.e. with taking into account the expansion for the convective velocity (28). However, if the problem of two bodies with large arbitrary penetration is considered, then the contact integral in the full form (33) together with the full convective velocity equations (23) must be used.

In the current contribution the further discussion is restricted to the non-frictional case, i.e. $T^i = 0$. The case with friction is considered in a following paper.

3.1 Penalty regularization.

The penalty regularization of the contact condition, see [19], [9], leads to the following regularized functional:

$$\delta W_c = \int_S \epsilon_N \langle g \rangle \delta g ds \tag{36}$$

where ϵ_N is a penalty parameter and $\langle\rangle$ are Macauley brackets, which means that the integral is computed only if the value of penetration g is nonpositive

$$\langle g \rangle = \begin{cases} 0, \ if \quad g > 0 \\ g, \ if \quad g \leq 0 \end{cases} .$$

The contact integral (36) is computed over the master surface. Within the "node-to-surface" approach the value of penetration is taken from the node and, in fact, there is no computation of the surface integral over the master surface. Following the velocity description, we take the full time derivative in order to linearize it as well as to develop the variation

$$D_v(\delta W_c) = \int_S \epsilon_N H(-g)(\dot{g} \ \delta g + g \ \delta \dot{g}) ds \tag{37}$$

where $H(-g)$ is the Heaviside function, replacing the Macauley brackets. An expression for the linearized penetration follows from the kinematical equation (25)

$$\dot{g} = \dot{\xi}^3 = (\mathbf{v}_s - \mathbf{v}) \cdot \mathbf{n}. \tag{38}$$

The full time derivative (see eqn. 18) is used to linearize the variation of the penetration (34)

$$D_v(\delta g) = \delta \dot{g} = -\delta \mathbf{r}_{,i} \dot{\xi}^i \cdot \mathbf{n} + (\delta \mathbf{r}_s - \delta \mathbf{r}) \cdot (\frac{\partial \mathbf{n}}{\partial t} + \mathbf{n}_i \dot{\xi}^i) =$$

$$= -(\delta \mathbf{r}_{,i} \cdot \mathbf{n}) a^{ij} (\mathbf{v}_s - \mathbf{v}) \cdot \mathbf{r}_{,j} - (\delta \mathbf{r}_s - \delta \mathbf{r}) \cdot \mathbf{r}_{,i} h^{ij} (\mathbf{v}_s - \mathbf{v}) \cdot \mathbf{r}_{,j} - (\delta \mathbf{r}_s - \delta \mathbf{r}) \cdot \mathbf{r}_{,i} a^{ij} (\mathbf{v}_i \cdot \mathbf{n}) \tag{39}$$

For this expression the Weingarten formula (9), the equation for the convective velocities (26) and the orthogonality condition $\mathbf{n} \cdot \mathbf{r}_{,i} = 0$ are taken into account. The complete linearization of the contact integral (36) leads to the following result

$$D(\delta W_c^N) =$$

$$= \int_S \epsilon_N \ H(-g) \ (\delta \mathbf{r}_s - \delta \mathbf{r}) \cdot (\mathbf{n} \otimes \mathbf{n})(\mathbf{v}_s - \mathbf{v}) ds - \tag{40}$$

$$- \int_S \epsilon_N \ H(-g) \ g \ \delta \mathbf{r}_{,j} \cdot a^{ij} (\mathbf{n} \otimes \mathbf{r}_{,i})(\mathbf{v}_s - \mathbf{v}) ds - \tag{41}$$

$$- \int_S \epsilon_N \ H(-g) \ g \ (\delta \mathbf{r}_s - \delta \mathbf{r}) \cdot a^{ij} (\mathbf{r}_{,j} \otimes \mathbf{n}) \mathbf{v}_{,i} ds - \tag{42}$$

$$- \int_S \epsilon_N \ H(-g) \ g \ (\delta \mathbf{r}_s - \delta \mathbf{r}) \cdot h^{ij} (\mathbf{r}_{,i} \otimes \mathbf{r}_{,j})(\mathbf{v}_s - \mathbf{v}) ds. \tag{43}$$

The full contact tangent matrix is then directly subdivided into the "main" part eq. (40) and the "curvature" part (41, 42, 43) which is small due to the small penetration g. The "curvature" part itself consist of a "rotational" part (eq. 41 and 42) and a "pure curvature" part (eq. 43). The "rotational" part contains derivatives of $\delta \mathbf{r}$ and $\mathbf{v}$ with respect to the convective coordinates ξ^j and, therefore, is responsible for the rotation of a contact surface during the incremental solution procedure. The pure curvature part contains components of the curvature tensor h^{ij} and, therefore, is responsible for the change of the master surface curvature.

4 Finite element discretization.

Though, all derivations and later numerical tests are provided also for elements based on higher order shape functions, in this section we consider only details of the finite element implementation for the bilinear element. All equations for the tangent matrix have an algorithmic structure and, therefore, the procedure of the tangent matrix derivation can be easily extended into any other case. The variables of the displacement field of the bilinear "contact element" are described by the vector

$$\mathbf{u}^T = \{u_1^{(1)}, u_2^{(1)}, u_3^{(1)}, u_1^{(2)}, u_2^{(2)}, u_3^{(2)}, u_1^{(3)}, u_2^{(3)}, u_3^{(3)}, u_1^{(4)}, u_2^{(4)}, u_3^{(4)}, u_1^{(5)}, u_2^{(5)}, u_3^{(5)}\}^T, \tag{44}$$

where the first 4 nodes belong to the master surface, while the 5'th node is the "slave" node.

Position matrices $\mathbf{A}^k$ of dimension 3×15, where the unit matrix 3×3 is on k'th position,

$$\mathbf{A}^k = \begin{bmatrix} 0 & 0 & 0 & \cdot & \cdot & \cdot & 1 & 0 & 0 & \cdot & \cdot & \cdot \\ 0 & 0 & 0 & \cdot & \cdot & \cdot & 0 & 1 & 0 & \cdot & \cdot & \cdot \\ 0 & 0 & 0 & \cdot & \cdot & \cdot & 0 & 0 & 1 & \cdot & \cdot & \cdot \end{bmatrix} \tag{45}$$

serve to define the variation of nodal displacements for the "master" surface as

$$\delta \mathbf{u}_k = \mathbf{A}^k \delta \mathbf{u} \tag{46}$$

and the variation of the "slave" node S as

$$\delta \mathbf{r}_s = \mathbf{A}^5 \delta \mathbf{u}, \tag{47}$$

therefore, the variation of the projection point C is defined as

$$\delta \mathbf{r} = \sum_{k=1}^{4} N_k \mathbf{A}^k \delta \mathbf{u} = \mathbf{A}^c \delta \mathbf{u}, \tag{48}$$

where $\mathbf{A}^c = \sum_{k=1}^{4} N_k \mathbf{A}^k$. Similar expressions can be given for the velocity vector. Using this notation, we will have

$$\delta \mathbf{r}_s - \delta \mathbf{r} = (\mathbf{A}^5 - \mathbf{A}^c)\delta \mathbf{u}. \tag{49}$$

The surface tangent vectors $\mathbf{r}_{,i}$ are defined by differentiation of the shape functions

$$\mathbf{r}_i = \sum_{k=1}^{4} \frac{\partial N_k(\xi^1, \xi^2)}{\partial \xi^i} \mathbf{x}^{(k)}. \tag{50}$$

The normal (4), the first (5) and the second fundamental tensor (7) can be then computed according to their definition.

After introducing a new matrix $\mathbf{A} = \mathbf{A}^5 - \mathbf{A}^c$

$$\mathbf{A} = \begin{bmatrix} -N_1 & 0 & 0 & -N_2 & 0 & 0 & -N_3 & 0 & 0 & -N_4 & 0 & 0 & 1 & 0 & 0 \\ 0 & -N_1 & 0 & 0 & -N_2 & 0 & 0 & -N_3 & 0 & 0 & -N_4 & 0 & 0 & 1 & 0 \\ 0 & 0 & -N_1 & 0 & 0 & -N_2 & 0 & 0 & -N_3 & 0 & 0 & -N_4 & 0 & 0 & 1 \end{bmatrix}, \tag{51}$$

the relative velocity vector $(\mathbf{v}_s - \mathbf{v})$ has the following form:

$$\mathbf{v}_s - \mathbf{v} = (\mathbf{A}^{(5)} - \mathbf{A}^c)\tilde{\mathbf{v}} = \mathbf{A}\tilde{\mathbf{v}}, \tag{52}$$

where $\tilde{\mathbf{v}}$ is a nodal velocity vector of the contact element, similar to the nodal displacement vector $\mathbf{u}$ (44). It has to be noted that the velocity $\mathbf{v}$ introduced for the tangent matrix derivation has to be treated as an incremental displacement $\Delta\mathbf{u}$ within the computation.

With the matrix of the shape function derivative $\mathbf{A}_{,j}$

$$\mathbf{A}_{,j} = \begin{bmatrix} N_{1,j} & 0 & 0 & N_{2,j} & 0 & 0 & N_{3,j} & 0 & 0 & N_{4,j} & 0 & 0 & 0 & 0 & 0 \\ 0 & N_{1,j} & 0 & 0 & N_{2,j} & 0 & 0 & N_{2,j} & 0 & 0 & N_{4,j} & 0 & 0 & 0 & 0 \\ 0 & 0 & N_{1,j} & 0 & 0 & N_{2,j} & 0 & 0 & N_{2,j} & 0 & 0 & N_{4,j} & 0 & 0 & 0 \end{bmatrix}, \tag{53}$$

the vectors $\delta\mathbf{r}_{,j}$ and $\mathbf{v}_{,j}$ are written as

$$\delta\mathbf{r}_{,j} = \mathbf{A}_{,j}\delta\mathbf{u}, \quad \mathbf{v}_{,j} = \mathbf{A}_{,j}\tilde{\mathbf{v}}. \tag{54}$$

The "main" part, often also called "constitutive" part, of the normal tangent matrix (40) has then the following form

$$\mathbf{K}^{(m)} = H(-g)\ \epsilon_N \int_S \mathbf{A}^T(\mathbf{n}\otimes\mathbf{n})\mathbf{A}ds \tag{55}$$

The "curvature" part of the tangent matrix, in the general case, consists of three matrices. The first two matrices (41) and (42) build the rotation matrix

$$\mathbf{K}_r^{(1)} = -H(-g)\ \epsilon_N \int_S g\ \mathbf{A}_{,j}^T a^{ij}(\mathbf{n}\otimes\mathbf{r}_{,i})\mathbf{A}ds \tag{56}$$

$$\mathbf{K}_r^{(2)} = -H(-g)\ \epsilon_N \int_S g\ \mathbf{A}^T a^{ij}(\mathbf{r}_{,i}\otimes\mathbf{n})\mathbf{A}_{,j}ds \tag{57}$$

and the third matrix (43) is the "pure curvature" matrix

$$\mathbf{K}^{(h)} = -H(-g)\ \epsilon_N \int_S g\ \mathbf{A}^T h^{ij}(\mathbf{r}_{,i}\otimes\mathbf{r}_{,j})\mathbf{A}ds \tag{58}$$

Thus, the full normal tangent matrix is set up as

$$\mathbf{K} = \mathbf{K}^{(m)} + \mathbf{K}^{(curv)} = \mathbf{K}^{(m)} + \mathbf{K}_r^{(1)} + \mathbf{K}_r^{(2)} + \mathbf{K}^{(h)} \tag{59}$$

which is symmetric due to $\mathbf{K}_r^{(1)^T} = \mathbf{K}_r^{(2)}$, and due to the symmetry of $h^{ij}(\mathbf{r}_{,i}\otimes\mathbf{r}_{,j})$.

The proposed procedure has been implemented into the finite element code FEAP-MeKA documented in [14] and [20].

5 Numerical examples.

In this section a series of numerical examples of contact problems between a flexible structure and rigid surfaces of second order (cylinder and sphere) are investigated. Bilinear and biquadratic contact elements are used for parameterization of both contact surfaces. The aim is to estimate the influence of rotational and curvature parts of the contact tangent matrix on the convergence of the iterative algorithm. In order to investigate the corresponding contribution of each part of the tangent matrix, the following three alternatives are considered

a. Use of the full tangent matrix $\mathbf{K} = \mathbf{K}^{(m)} + \mathbf{K}^{(curv)}$.

b. Use the main part $\mathbf{K}^{(m)}$ and the rotational part $\mathbf{K}_r$,
i.e. the contact matrix $\mathbf{K} = \mathbf{K}^{(m)} + \mathbf{K}_r^{(1)} + \mathbf{K}_r^{(2)}$.

c. Use the main part $\mathbf{K}^{(m)}$ and the pure curvature part $\mathbf{K}^h$, i.e. the contact matrix $\mathbf{K} = \mathbf{K}^{(m)} + \mathbf{K}^{(h)}$.

d. Use only the main part $\mathbf{K}^{(m)}$ as a contact matrix, i.e. $\mathbf{K} = \mathbf{K}^{(m)}$

The main contribution into the full contact tangent matrix comes usually from the main matrix $\mathbf{K}^{(m)}$, therefore a relative measure ε is chosen as an estimate

$$\varepsilon = \frac{||\mathbf{K} - \mathbf{K}^{(m)}||}{||\mathbf{K}^{(m)}||} \cdot 100\% \tag{60}$$

with the following matrix norm:

$$||K|| = \max_i \sum_{j=1}^{n} |k_{ij}| \tag{61}$$

The influence on the convergence rate is given by the number of equilibrium iterations at each load step, while the value ε, computed at each load step after the equilibrium iteration, is given in order to estimate the contribution of the "curvature" part.

5.1 Bending of a beam over a rigid cylinder

5.1.1 Linear approximation of the contact surfaces

A clamped elastic beam is loaded by prescribed displacements at the free end in vertical direction, that leads to bending over a rigid cylinder. The parameters of the beam are chosen as: length l=24 cm, height h=0.25 cm, width b=1 cm; the material model is St. Venant elastic material with an elasticity modulus of $1.0 \cdot 10^4$; the Poisson ratio is 0.3; for contact a penalty factor of $1.0 \cdot 10^4$ MPa/cm is chosen. The beam is modeled with 24 "solid-shell" elements [4] with linear shape functions plus some added shell specific enhancements. The rigid cylinder with radius R=2 cm is modelled with 49 contact elements in the circumferential direction. The central axis of the cylinder is positioned at 12 cm from the clamping. For the contact elements a linear approximation for the contact surfaces is used; the beam surface was treated as a "master" surface. The prescribed final displacement $u_{ext} = 9$ cm is subdivided into 90 identical load steps. Fig. 2 shows a sequence of the deformed beam during loading at the 0, 20, 40, 60, 80 and 90'th load step respectively. The value of penetration does not exceed 0.18 % of the beam thickness.

The results of the computation are presented in table 1. The convergence rate in each load step is estimated by the number of equilibrium iterations (column *No. it. / l.s.* in table 1), which has been changing over load steps, e.g. the computation shows 3 equilibrium iterations per load step within the first 15 load steps. The contribution of various parts of the tangent matrix is estimated by the norm in eq. (60).

We obtain 319 total iterations for the cases **a** and **b** and 345 iterations for the cases **c** and **d**. As expected, there is no difference between the results if the "pure curvature" part is taken into account or not, because the curvature tensor is zero. It is also obvious that the rotational part is much more important.

5.1.2 Quadratic approximation of the contact surfaces.

Now the beam from the previous example is modeled with 12 quadratic "solid-shell" elements [5]. The penalty factor is chosen as $5.0 \cdot 10^4$ MPa/cm, which leads to a maximum penetration of 0.048 % of the beam thickness.

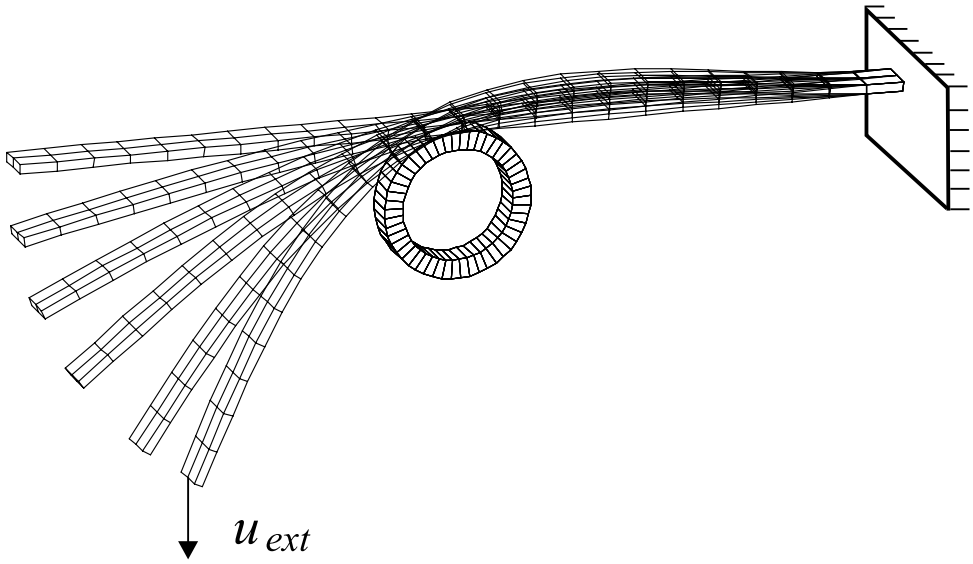

Figure 2: Bending of a clamped beam over a rigid cylinder. Sequence of deformations.

The total number of iterations for case **a** with full matrix and case **b**, when the rotational matrix is taken into account, is identical, therefore, table 2 presents the influence of the "curvature" matrix on convergence in case of **a**, **c** and **d**. Though, elements with quadratic shape functions are used, the influence of the "pure curvature" part is still negligible. It is even possible to obtain the result with the main matrix only with a loss of 7 % of the total number of iterations.

5.2 Bending of a beam over a rigid sphere.

A more general case to examine the influence of all parts of the contact matrix is to consider the contact with a body with a curvature in both directions.

The clamped elastic beam of the previous example, but with a width of $b = 4$ cm, is now bending over a rigid sphere. The radius of the sphere is 4 cm. The center of the sphere is positioned at 0.5 cm from the edge of the beam and at 12 cm along the beam measured from the clamping. The rigid sphere was modeled with 512 bilinear contact elements. The contact elements of the beam inherit the geometry of the beam and, therefore, have biquadratic approximations; the beam surface is represented as a "master" surface. Two asymmetric forces $F_1 = 17.5$ N and $F_2 = 70$ N are applied in the nodes at the free end as presented in Fig. 3. In the computation they were applied incrementally with 100 identical load steps. Fig. 3 shows the evolution diagram of the deformation for the 0, 20, 40, 60, 80, 100'th load step respectively. In this example we have bending and twisting of the beam as well.

Again the composition of the tangent matrix is varied. The value of the contact penalty is taken as $0.5 \cdot 10^4$ MPa/cm for the cases **c** and **d**, but $0.5 \cdot 10^3$ MPa/cm for the cases **a** and **b** due to convergence problems. The last value leads to a maximum penetration of 0.75 % of the beam thickness. Table 3 shows the result of the analysis.

In this case the curvature is changing in both directions and, as it can be seen from the result for case **b**, the influence of the "rotational" and the "pure curvature" part is larger. The higher the curvature, the more equilibrium iterations are necessary. One can see that the influence of the "rotational" part in this example is crucial, because the exclusion of the "rotational" part leads to an increase of the total number of iterations of more than 40 % , while the influence of the "pure curvature" part is still small. For the case **c**, which is not presented in the table 3, we

obtain 609 iterations. For the full matrix (case **a**), however, the computation of the curvature part is rather costly in comparison with the "main" and with the "rotational" part, due to the necessity to compute the second derivative and the double summation for the contravariant components of the curvature tensor h^{ij}, see eqn. (8). Thus it appears to be the most efficient choice to consider the analysis without "pure curvature" matrix.

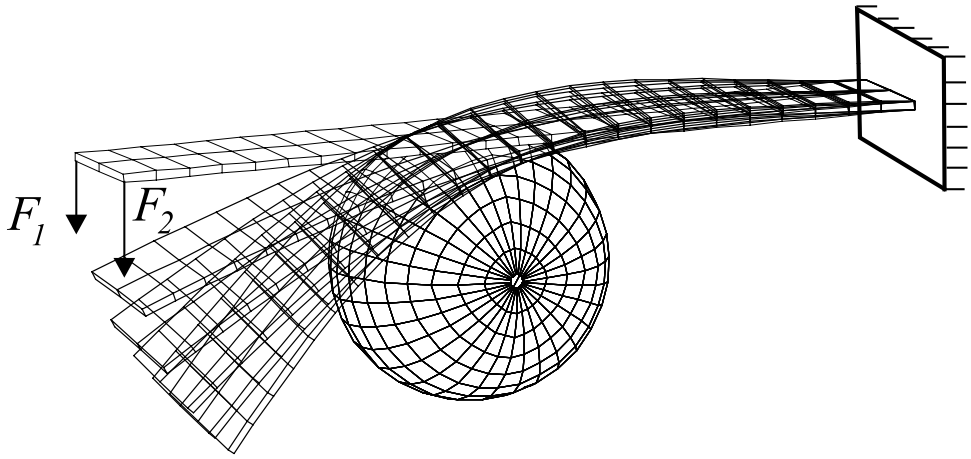

Figure 3: Bending of a beam over a rigid sphere. Sequence of deformations.

6 Conclusions

In this contribution a velocity description for the development of a consistent contact tangent matrix has been proposed. It allows to distinguish between three parts of a tangent matrix, namely the "main" part, the "rotational" part and the "pure curvature" part.

The numerical examples show that in the case of linear approximations and aligned contact elements keeping of the "pure curvature" part is meaningless. Then, it even appears sufficient to keep only the main part as a contact tangent matrix.

If elements with higher order approximations are used, the influence of the "rotational" part is larger, but the influence of the "pure curvature" part remains still small. Therefore, the last part, which is computationally more expensive then the others, can be eliminated from the complete tangent matrix without loss of efficiency.

References

[1] Bonet J., Wood R.D. (2000) Nonlinear continuum mechanics for finite element analysis. Cambridge Univ. Press, Cambridge.

[2] Gray A. (1993) Modern differential geometry of curves and surfaces. CRC Press, Boca Raton.

[3] Hauptmann R., Schweizerhof K. (1998) A systematic development of 'solid-shell' element formulation for linear and non-linear analysis employing only displacement degrees of freedom. *International Journal for Numerical Methods in Engineering*, **42**, pp. 49-69.

[4] Hauptmann R., Schweizerhof K., Doll S. (2000) Extension of the 'solid-shell' concept for applications to large elastic and large elastoplastic deformations. *International Journal for Numerical Methods in Engineering*, **49**, pp. 1121-1141.

[5] Hauptmann R., Doll S., Harnau M., Schweizerhof K. (2001) "Solid-shell" elements with linear and quadratic shape functions at large deformations with nearly incompressible materials. *Computers & Structures*, **79**, pp. 1671-1685.

[6] Kikuchi N., Oden J.T. (1988) Contact problems in Elasticity: A Study of Variational Inequalities and Finite Element Methods, SIAM, Philadelphia.

[7] Laursen T.A. (1992) Formulation and treatment of frictional contact problems using finite elements. Dissertation, SUDAM Report No. 92-6, Stanford University.

[8] Laursen T.A., Simo J.C. (1993) A continuum-based finite element formulation for the implicit solution of multibody large deformation frictional contact problems. *International Journal for Numerical Methods in Engineering*, **35**, pp. 3451-3485.

[9] Laursen T.A. (2002) Computational Contact and Impact Mechanics. Fundamentals of Modeling Interfacial Phenomena in Nonlinear Finite Element Analysis, Springer, Berlin Heidelberg New York.

[10] Marsden J.E., Hughes T.J.R. (1983) Mathematical foundations of elasticity. Prentice-Hall, Englewood cliff, NJ.

[11] Parisch H. (1989) A consistent tangent stiffness matrix for three-dimensional nonlinear contact analysis. *International Journal for Numerical Methods in Engineering*. **28**, pp. 1803-1812.

[12] Pietrzak G., Curnier A. (1999) Large deformation frictional contact mechanics: continuum formulation and augmented Lagrangian treatment. *Computer Methods in Applied Mechanics and Engineering*. **177**, pp. 351-381.

[13] Simo J.C., Laursen T.A. (1992) An augmented Lagrangian treatment of contact problems involving friction. *Computers & Structures*. **42**, pp. 97-116.

[14] Taylor R.L. (1987) FEAP – A Finite Element Analysis Program. University of California at Berkeley, Berkeley. Schweizerhof, K. and Coworkers, FEAP - Mechanik - Karlsruhe, Institut für Mechanik, Universität Karlsruhe.

[15] Wriggers P., Simo J.C., Taylor R.L. (1985) Penalty and augmented Lagrangian formulations for contact problems. In: Middleton J., Pande G.N. (eds), Proceeding NUMETA Conference, Balkema, Rotterdam.

[16] Wriggers P., Simo J.C. (1985) A note on tangent stiffness matrices for fully nonlinear contact problems. *Communication in Applied Numerical Methods*, **1**, pp. 199-203.

[17] Wriggers P., Vu Van, Stein E. (1990) Finite element formulation of large deformation impact-contact problems with friction. *Computers & Structure>s*, **37**, pp. 319-331.

[18] Wriggers P. (1995) Finite element algorithm for contact problems. *Archives of Computational Methods in Engineering*, **2(4)**, pp. 1-49.

[19] Wriggers P. (2002) Computational Contact Mechanics. John Wiley & Sons.

[20] Zienkiewicz O. C., Taylor R. L. (2000) Finite Element Method: Volume 1, The Basis. 5th edn. Butterworth-Heinemann, New York.

Tables.

Case a/b				Case c/d		
No. l.s.	No. it./l.s.	Cum. No. it.	$\varepsilon \cdot 10^{-2}$ % eq. (60)	No. l.s.	No. it./l.s.	Cum. No. it.
1-15	3	45	0.18	1-15	3	45
16	5	50	0.19	16	5	50
17-45	3	137	0.55	17-26	3	80
46-73	4	249	0.45	27-73	4	268
74	5	254	0.62	74	5	273
75	4	258	1.04	75	4	277
76	5	263	0.62	76	5	282
77-90	4	319	1.26	77-83	4	310
				84-90	5	345

Table 1: Bending over a rigid cylinder. Bilinear elements for the beam. Node-to-surface contact elements. Influence of various contact stiffness parts on convergence. Case a: full matrix, case b: without curvature part; case c: without rotational part; case d: only main matrix. Comparison of no. of iterations in each load step (l.s.) and accumulated over several load steps.

Case a/b				Case c				Case d		
No. l.s.	No. it./l.s.	Cum. No. it.	$\varepsilon \cdot 10^{-2}\%$	No. l.s.	No. it./l.s.	Cum. No. it.	$\varepsilon \cdot 10^{-4}$ %	No. l.s.	No. it./l.s.	Cum. No. it.
1-16	3	48	0.19	1-16	3	48	0.09	1-16	3	48
17-18	4	56	0.19	17-18	4	56	0.12	17-18	4	56
19-46	3	140	0.55	19-30	3	92	0.35	19-30	3	92
47	4	144	0.45	31-47	4	160	0.49	31-47	4	160
48-50	3	153	0.62	48	3	163	1.03	48	3	163
51-69	4	229	1.04	49-86	4	315	4.81	49-69	4	247
70	5	234	0.63	87-90	5	335	9.76	70	5	252
71-86	4	298	1.27					71-86	4	316
87	5	303	2.00					87	6	322
88-90	4	315	2.37					88-90	5	337

Table 2: Bending over a rigid cylinder. Biquadratic elements for the beam. Node-to-surface contact elements. Influence of various contact stiffness parts on convergence. Case a: full matrix; case b: without curvature part; case c: without rotational part; case d: only main matrix. Comparison of no. of iterations in each load step (l.s.) and accumulated over several load steps.

Case a				Case b			Case d		
No. l.s.	No. it./l.s.	Cum. No. it.	$\varepsilon \cdot 10^{-2}$ %	No. l.s.	No. it./l.s.	Cum. No. it.	No. l.s.	No. it./l.s.	Cum. No. it.
1	27	27	0.731	1	27	27	1	20	20
2-23	4	115	7.382	2-22	4	111	2-8	4	48
24	6	121	18.08	23	6	117	9-23	5	123
25-33	4	157	16.26	24-33	4	157	24	6	129
34	5	162	12.20	34	6	163	25-33	5	174
35-100	4	426	17.32	35-100	4	427	34-48	6	264
							49-58	5	314
							59-68	6	374
							69-85	7	493
							86-100	8	613

Table 3: Bending over a rigid sphere. Biquadratic elements for the beam. Node-to-surface contact elements. Influence of various contact stiffness parts on convergence. Case a: full matrix; case b: without curvature part; case d: only main matrix. Comparison of no. of iterations in all load steps (l.s.)